# Some Nonlinear Properties of Electron-Hole Plasmas Sustaining the Helical Instability

BETSY ANCKER-JOHNSON
*Boeing Scientific Research Laboratories, Seattle, Washington*
(Received 13 April 1964)

Electron-hole plasmas in $p$-InSb are driven far beyond the threshold of the helical instability into the nonlinear region by applying axial magnetic fields $B$ much greater than the threshold fields $B_{th}$. While the plasma is immersed in a *static* $B$ three fundamental properties of the plasma, namely the electric-field strength $E$ sustained in the plasma, the self-magnetic field $B_h$ produced by the rotating plasma, and the frequency of helical oscillations $f$, are measured. As $B$ is increased from zero, $E$ first decreases until $B=B_{th}$; then $E$ rises with a slope and magnitude greater than those associated with the decrease. The quantity $B_hR/I_T$, where $I_T=$ total current and $R=$radius, possesses a maximum as a function of $BR$. At constant $I_T$, $f$ exhibits a trend to increase with increasing penetration into the nonlinear region until the onset of turbulence; however, $f$ is a nonmonotonic function of $B$. $E$ is also measured while the plasma is immersed in a *magnetic field varying with time* at a rate $\dot{B}$. The most striking result is the splitting of the $B_{th}$ into two branches with increasing $\dot{B}$ as observed by the occurrences of two minima in the $E$ versus time curves. Comparisons are made among all these results and those available on the nonlinear properties of electron-ion plasmas, both experimental and theoretical.

## I. INTRODUCTION

THE helical instability at its threshold is a relatively well understood phenomenon in both electron-ion and electron-hole plasmas (see Ref. 1 for bibliography). Its nonlinear properties in electron-ion plasmas (positive column) beyond threshold, well into the supercritical region have been investigated as follows: The electric-field strength $E$ necessary to sustain the discharge rises rapidly with magnetic-field strength $B$ when $B$ is increased just beyond the threshold $B_{th}$ and the resulting enhancement in $E$ tends toward saturation for $B$ somewhat larger than $B_{th}$.[2] Then the plasma is turbulent but at several times $B_{th}$ the plasma can become homogeneous again.[3] The frequency of oscillations increases for $B>B_{th}$ preceding turbulence.[4] The internal magnetic field produced by a finite amplitude helix is typically $<1$ mG and has a maximum at a given $B>B_{th}$.[5] A nonlinear theory has been worked out by Holter and Johnson[6] treating the finite amplitude helix and Kadomtsev[7] has developed a theory of turbulence.

The following information has been reported about the nonlinear properties of the helical instability in electron-hole plasmas: Ivanov and Ryvkin[8] at the first observation of the effect in a semiconductor noted qualitatively that both the frequency and amplitude of oscillations increase with $E>E_{th}$ and less sharply with $B>B_{th}$. Ancker-Johnson[9] showed that the $E$ necessary to maintain a given current increases markedly at magnetic-field magnitudes just beyond $B_{th}$ and that the frequency and amplitude are not monotonic functions of $B>B_{th}$. A large hysteresis in the threshold conditions before and after an excursion into the supercritical region has been discovered.[10] The magnitudes of the magnetic field produced by well-developed helices have been determined and novel, displaced-loop $B$-$H$ curves presented.[1] These loops are surprisingly large—up to 165 Oe on a side. A nonlinear theory applicable to electron-hole plasmas is not yet available.

Time-dependent magnetic and electric fields have been used to suppress the helical instability in electron-ion plasmas. Both experimentally and theoretically Johnson and Jerde[11] have shown that $B_{th}$ is enhanced with increasing $dB/dt$. Rugge and Pyle[12] applied an unidirectional alternating $E$ and found a postponement of $B_{th}$ to higher values with increasing frequency greater than the growth rate of the instability.

This paper reports systematic measurements of several nonlinear properties of electron-hole plasmas sustaining the helical instability using both static and time-dependent magnetic fields to drive the instability into the supercritical region.

## II. EXPERIMENTAL DETAILS

Eight single-crystal samples of $p$-InSb were investigated. Their initial conductivity $\sigma$ ranges from 0.35 to 0.67 $(\Omega\ \text{cm})^{-1}$ and their mobility $\mu_p=R_H\sigma$ from 6000 to

[1] B. Ancker-Johnson, Phys. Rev. **135**, A1465 (1964).
[2] B. Lehnert, in *Proceedings of the Second United Nations International Conference on the Peaceful Uses of Atomic Energy, Geneva, 1958* (United Nations, Geneva, 1958), Vol. **32**, p. 239; F. C. Hoh and B. Lehnert, Phys. Fluids **3**, 600 (1960).
[3] H. S. Robertson, Bull. Am. Phys. Soc. **9**, 316 (1964).
[4] A. R. Akhmedov and A. A. Zaitsev, Zh. Techn. Fiz. **33**, 177 (1963); [English transl.: Soviet Phys.—Tech. Phys. **8**, 126 (1963)]; F. Bottiglioni, M. Fumelli and F. Prevot, in *Proceedings of the Sixth International Conference on Ionization Phenomena in Gases*, edited by P. Hubert and E. Cremieu-Alcan (S.E.R.M.A.), (Paris, 1963), Vol. II, p. 427.
[5] R. R. Johnson, in *Proceedings of the Sixth International Conference on Ionization Phenomena in Gases*, edited by P. Hubert and E. Cremieu-Alcan (S.E.R.M.A.), (Paris, 1963), Vol. I, p. 413.
[6] Ø. Holter and R. R. Johnson, Phys. Fluids (to be published).
[7] B. B. Kadomtsev, Zh. Techn. Fiz. **31**, 1273 (1961); (English transl.: Soviet Phys.—Tech. Phys. **6**, 927 (1961)].
[8] I. L. Ivanov and S. M. Ryvkin, Zh. Tech. Fiz. **28**, 774 (1958); English transl.: Soviet Phys.—Tech. Phys. **3**, 722 (1958)].
[9] B. Ancker-Johnson, in *Proceedings of the International Conference on Physics of Semiconductors* (Institute of Physics and the Physical Society, London, 1962), p. 141.
[10] B. Ancker-Johnson, Appl. Phys. Letters **3**, 104 (1963). H. S. Robertson has observed a similar type of hysteresis in a cesium arc plasma (private communication).
[11] R. R. Johnson and D. A. Jerde, Phys. Fluids **7**, 103 (1964).
[12] H. F. Rugge and R. V. Pyle, Phys. Fluids **7**, 754 (1964).

8600 cm²/V-sec at 77°K, the lattice temperature throughout these measurements ($R_H$=Hall constant). All are in the form of parallelepipeds of essentially square cross section with sides varying between 0.5 and 1.0 mm. Each is uniform to within ±5% down its length which ranges between 4 and 12 mm, as judged by standard conductivity and Hall measurements.

The plasma is produced by forcing current greater than Ohmic through the samples in the form of square waves with 1 to 8-μsec duration, depending on the particular measurement. The source resistance is 50 Ω. Variations on top of the square-wave input pulse are less than 4%; in fact undetectable even when a Tektronix Z plug-in comparator is used to expand the sensitivity of the oscilloscope by a factor of 10, e.g., from 2.5 to 0.25 V/div.

An axial magnetic field is provided by a 300-turn solenoid of diameter barely larger than that of the samples with which used. The current through the solenoid is fed to the $y$ plates of a sampling storage oscilloscope and varied to produce direct plots of the $E$ dependence on $B$. The oscilloscope was modified to operate at repetition rates as low as 30 cps, the rate used in this work to avoid heating the samples. A magnetic field with various rates of rise is obtained by driving the solenoid with a triangular-wave current pulse.

## III. EXPERIMENTAL RESULTS

### A. Static Magnetic Field

Figures 1(a) and 2(a) display the dependence, in two samples, of $E$ on $B$ for various initial levels of $E$. Each minimum in $E$ defines the corresponding $B_{th}$. Beyond it the helical instability oscillations occur. They do not appear to be very regular in this presentation because each trace is the result of a sampling of thousands of pulses. As $B$ is increased, $E$ at first decreases rather gradually to $-\Delta E$ and then more rapidly increases to a $+\Delta E > |-\Delta E|$. These data are plotted in Figs. 1(b) and 2(b). The rate-of-change of $E$ with respect to $B$ is always greater at $B > B_{th}$ than at $B < B_{th}$ (i.e., $+dE/dB > |-dE/dB|$) and for most of the range of $E$ over which the instability occurs, it is much greater, Fig. 1(b). Also, Fig. 1(b) shows that $+\Delta E$ is much greater than $|-\Delta E|$ in the range of $E$ for which the instability is most impressive, i.e., the upper traces in Fig. 1(a). Figure 2(b) shows in more detail the dependencies of $|\pm\Delta E|$ and $E_0$ on $B_{th}$ over a smaller range of the latter; in particular it clarifies that the maximum in $|-\Delta E|$ at intermediate $B_{th}$ values is real.

Some properties of the frequency of the helical instability oscillations as a function of $B$ are shown in Fig. 3. The results for the highest and lowest currents at which the oscillations can be readily observed in a particular sample are displayed. The frequency is a nonmonotonic function of $B$. At low currents, approaching Ohmic, the oscillations have vanishing amplitude as the plasma density approaches zero. At high currents the range in $B$ over which regular oscillations occur becomes vanishingly small. At sufficiently high currents the oscillations acquire a turbulent appearance. Figure 3 indicates that there is a general tendency for higher frequency oscillations to be associated with lower currents, but then larger $B$ is required. The $f$ at the lowest $B$ in the two cases plotted is the frequency at threshold. Over most of the frequency ranges $f$ is linear in $B$, in spite of the nonmonotonicity.

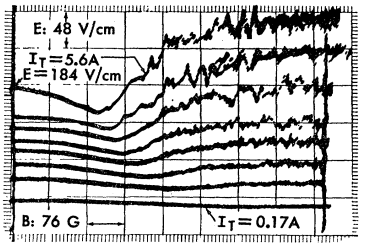


(a)

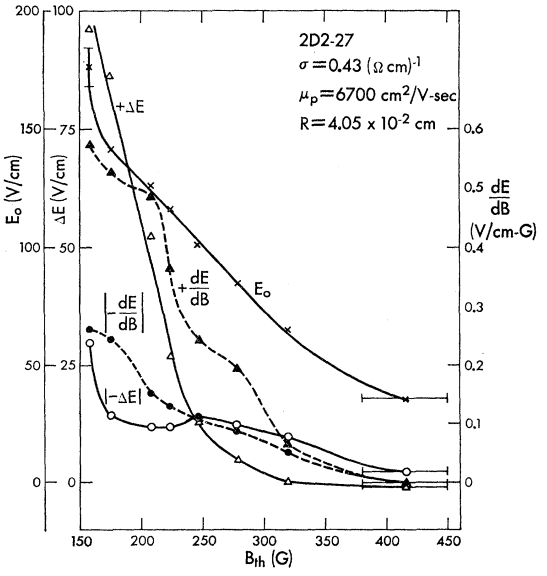


(b)

FIG. 1. The dependence of $E$ on $B$ for sample 2D2-27. (a) Oscillogram showing this dependence for 8 initial levels of $E$. (b) The initial magnitude of electric-field strength $E_0$; the positive and negative rate of change of $E$ with respect to $B$ occurring after and before $B_{th}$, respectively; and the increment and decrement in field strength occurring after and before $B_{th}$, respectively, all as a function of the helical instability threshold, $B_{th}$.

The finite amplitude helix produces an axial magnetic field in addition to the applied one. Data previously obtained[1] are cast into forms in Figs. 4 and 5 suitable for qualitative comparisons with the nonlinear theory[6] applicable to electron-ion plasmas. (See Sec. IV.) Figure 4 shows that the self-magnetic field produced by the helix divided by the total current (which is different for each plotted point) has a maximum as a function of applied $B$. (The applied $B$ is actually $B_{th}$ for each

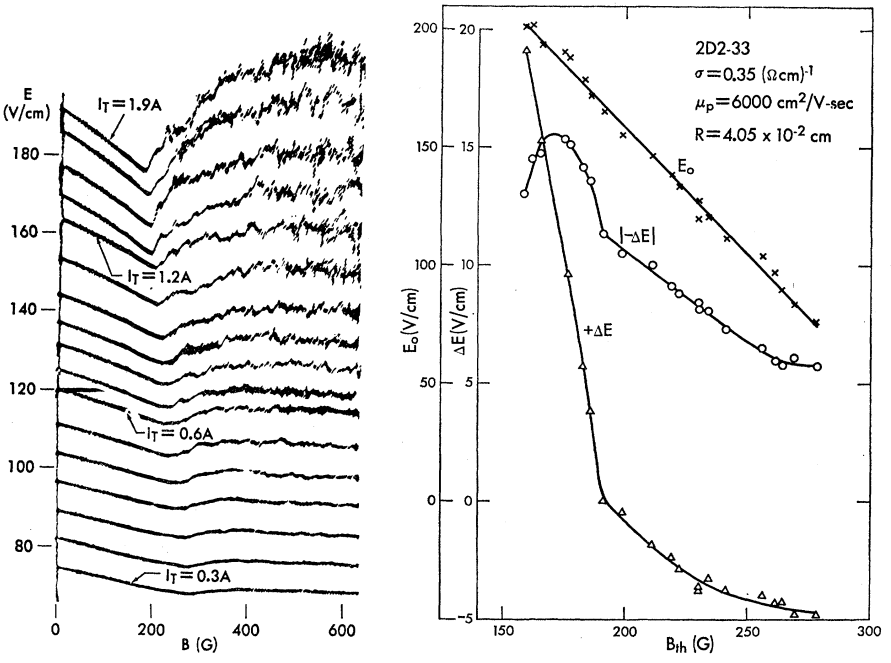


FIG. 2. The dependence of $E$ on $B$ for sample 2D2-33. (a) Oscillogram showing this dependence for 17 initial levels of $E$. (b) More detailed measurements of $|\pm\Delta E|$ than are shown in Fig. 1(b).

plotted point.) The total current ranged from 10.6 to 0.1 A in the four samples of Fig. 4.

As a result of the helix self-$B$, an hysteresis in the threshold conditions of the instability is observed.[1,10] These hysteresis electric and magnetic-field strengths can be as much as 55% of their respective threshold magnitudes, Fig. 5. Both $E_{hys}$ and $B_{hys}$ approach zero as the current in the sample is decreased to the Ohmic range and hence the plasma density vanishes. Fig. 5 shows that the ratio of $E_{hys}/E_{th}$ to $B_{hys}/B_{th}$ lies between 1 and 2.

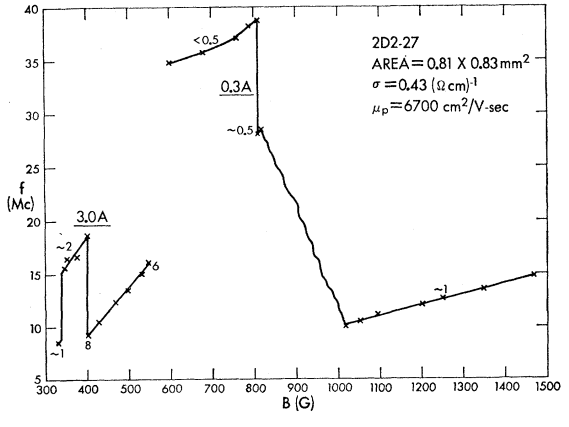


FIG. 3. The frequency of oscillations as a function of applied magnetic field for the highest and lowest currents at which these oscillations are readily observable in this sample. The numbers which are not underlined indicate the amplitude of oscillations in V/cm.

## B. Time-Dependent Magnetic Field

Some voltage responses associated with particular $dB/dt$ values are recorded in Figs. 6–8. In Fig. 6 the dips in $E$, $|-\Delta E|$, signifying stabilization of the plasma, are shown for seven different $dB/dt$ values. Each minimum in $E$ defines the corresponding $B_{th}$ and for $B>B_{th}$ the electric-field strength rises steeply. Such behavior also results when a static $B$ is applied (cf. the $E$-$B$ plots of Figs. 1(a) and 2(a). A new phenomenon attributable to the time-dependent nature of the applied $B$ is the splitting of some minima into two parts. The larger $dB/dt$ is, beyond a threshold, the more widely separated

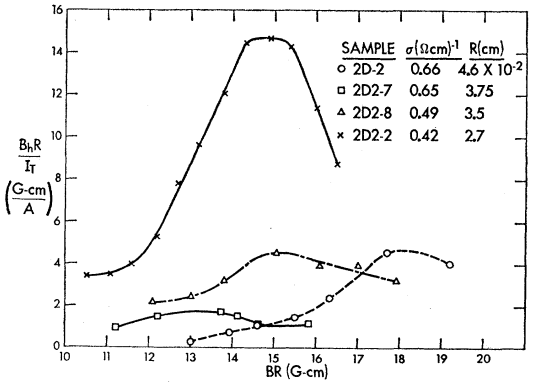


FIG. 4. The magnetic field produced by the helix is shown as a function of applied magnetic field. $R$=distance from the center of the sample cross section to the nearest surface. $I_T$=total current carried by the sample.

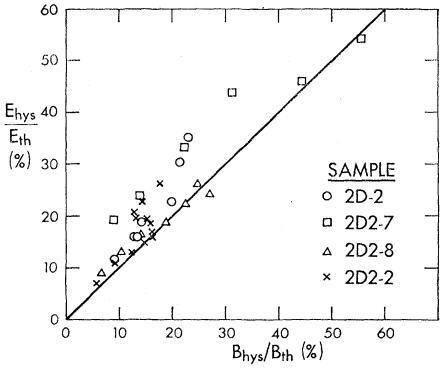


FIG. 5. The ratio of the magnitude of the hysteresis electric-field strength associated with the finite amplitude helix to its threshold value as a function of the ratio of the magnetic field produced by the helix to its threshold. The line serves to show that the former ratio is equal to or larger than the latter within a factor of 2.

in $B$ are the two minima. Figure 7 portrays this effect in another sample in more detail at relatively large $dB/dt$ values. The helical instability oscillations probably commence as $E$ rises after the first minimum and then vanish as the second minimum is approached to reappear during the steep rise in $E$ to $+\Delta E$. Since the helical instability oscillations are in the tens of Mc/sec range for the plasmas used in the present study and the sweep rate facilitating clear resolution of the peaks is 0.1 $\mu$sec/cm the last statement has not been proved.

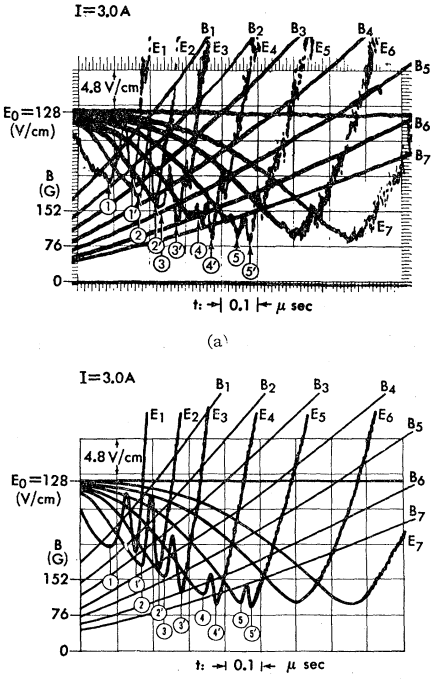


FIG. 6. Oscillograms (a) and simplified sketch of same (b) showing the simultaneous recording of $B$ and $E$ as a function of time in sample 2D2-27. The two minima in $E$ traces No. 1 to 5 are labeled 1, 1′ for $E_1$, etc.

The dual nature of the instability threshold as a function of $dB/dt$ is shown in Fig. 9 using data from many oscillograms like Figs. 7 and 8. No such duality in $B_{th}$ is observed if the plasma density is too low, e.g., for an $I_0$ one-half the magnitude used to obtain the data of Fig. 9, no splitting occurred. The $dB/dt$ threshold for this effect is $\sim$175 G/$\mu$sec in both the samples studied in detail for current levels of 2.5 to 3.0 A. As Fig. 9 indicates, the separation in $B$ of the splitting saturates at large $dB/dt$ values.

The $E$ response beyond, as well as before, $B=B_{th}$ is shown in Fig. 8, i.e., the sensitivities of all the scales are reduced compared to Fig. 7. As also noted in the static $B$ studies [Fig. 1(b)], the destabilizing enhancement in $E$, $+\Delta E$ is much larger than $|-\Delta E|$. The latter varies from 13 to 2 V/cm in the $dB/dt$ region from 100 to 1300 G/$\mu$sec under the conditions of Fig. 9, and in the other sample (that of Fig. 6) from 19 to 9 V/cm for

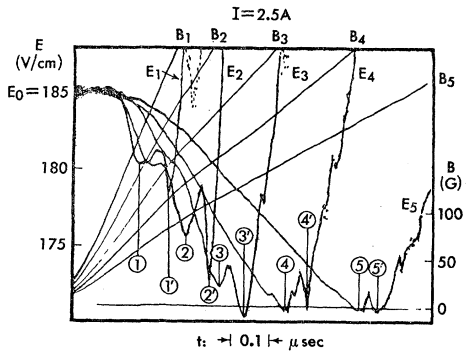


FIG. 7. Oscillograms showing the simultaneous recording of $B$ and $E$ as a function of time in sample 2D2-33. The two minima in $E$ traces No. 1 to 5 are labeled 1, 1′ for $E_1$, etc. (The improvement in focus compared with Fig. 6 was accomplished by modifying the sampling storage oscilloscope.)

$dB/dt$ from 50 to 900 G/$\mu$sec when $I_0$=3.0 A. $|-\Delta E|$ saturates at its maximum when $dB/dt$ is relatively small as Figs. 6–8 show. In contrast, $+\Delta E$ saturates with increasing $B$ independent of $dB/dt$, at least over the range $370<dB/dt<800$ G/$\mu$sec under the conditions of Fig. 9. Saturation of $+\Delta E$ required $B\approx 2B_{th}$.

The oscillogram of Fig. 10 serves to summarize some of the results of applying either a static $B$ or one which rises constantly with time. The conditions correspond to those of the second $E$ (and $B$) traces from the left in Fig. 6. The duality of $B_{th}$ found only in a $B$ that is increasing in time is just resolved. $|-\Delta E|=12$ V/cm, whereas $+\Delta E$ is four times as large. The slope $|-dE/dB|<dE/dB$. The quantity $+\Delta E$ saturates at $B\approx 2B_{th}$. The corresponding current response is also shown in this oscillogram.

The results reported so far all concern the driving of a plasma from its quiescent stable state to a rotating unstable one. In the following the response of a plasma as it makes the transition in the other direction, namely,

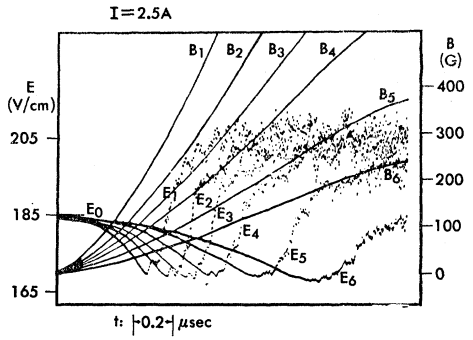


FIG. 8. More plots like those of Fig. 7 taken on compressed scales to illustrate the saturation of $|\pm\Delta E|$.

from its unstable to stable state is considered. A comparison of the $E$ response for the transition in each direction is afforded by Fig. 11. It is immediately apparent that the threshold between stability and instability occurs at a lower $B$ in the $-dB/dt$ case. Also, the amount of stabilization as measured by $|-\Delta E|$ is greater. A series of such oscillograms for varying $|\pm dB/dt|$ yields the information in Fig. 12. For comparison the $B_{\text{th}+}$ values for the transition from stable to unstable plasma are taken from Fig. 9; the present series of measurements reproduced the top branch. The line representing the $|-\Delta E|_+$ values, shown also for comparison, is the average of measurements used to produce Fig. 9 (i.e., data from oscillograms such as Figs. 6–8) and the present data. The lower two curves in Fig. 12 show the results for the transition from an

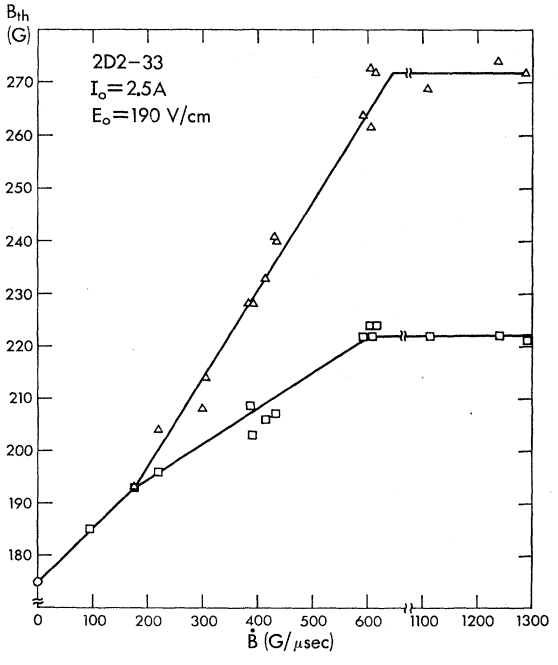


FIG. 9. The helical instability threshold in a magnetic field which is constantly increasing with time. The point for $dB/dt=0$ is taken from Fig. 2(b).

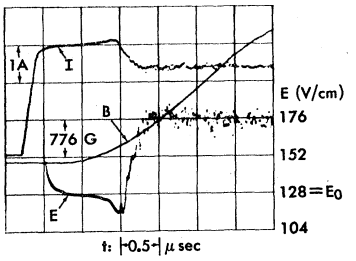


FIG. 10. Oscillogram of $I$, $E$, and $B$ as a function of time taken with an ordinary fast-response oscilloscope, i.e., nonsampling.

unstable to a stable plasma. The $B_{\text{th}-}$ are not only much smaller than the $B_{\text{th}+}$ but decrease, rather than increase with enhanced $|dB/dt|$. For relatively small values of $|-dB/dt|$, the $|-\Delta E|_-$ values are larger than those occurring in a rising $B$ (cf. Fig. 11); however over most of the $dB/dt$ range, the reverse occurs. No duality in $B_{\text{th}-}$, in contrast to $B_{\text{th}+}$, could be observed.

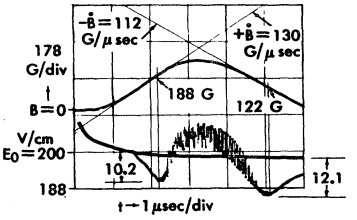


FIG. 11. Oscillogram illustrating the $E$ response when the $B$ first increases in time and then decreases (upper trace). The $E$ response in the absence of applied $B$ is superimposed on the response (lower trace) when the $B$ is applied. Sample 2D2-33.

## IV. DISCUSSION

The curves of Figs. 1(a) and 2(a) are similar to those reported earlier by the author,[9] but the present experi-

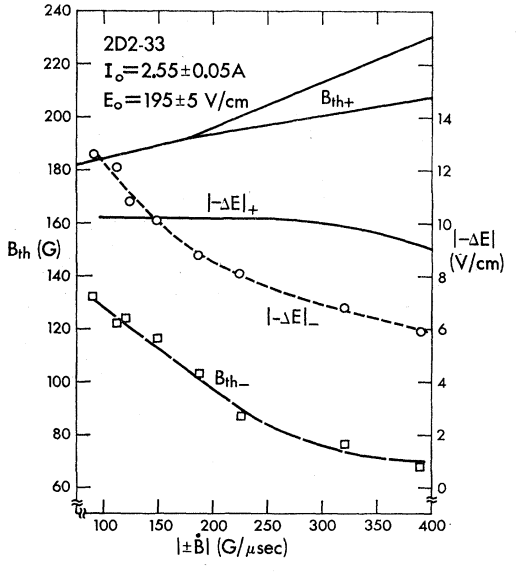


FIG. 12. The threshold magnetic fields and decrements in electric-field strengths therewith produced, as a function of a constantly rising and also falling with time applied $B$. The lower two curves show the results as a function of $-dB/dt$.

mental method enables accurate ascertainment of much more detail, Figs. 1(b) and 2(b). It is now clear that an axial $B<B_{th}$ produces a decrement in $E$, thereby indicating that the plasma is stabilized as is the case in electron-ion plasmas (cf. Ref. 2(b), Fig. 3). This decrement increases as $B$ approaches $B_{th}$ [cf. Fig. 1(a) and 2(a)] but is largest at small values of $B=B_{th}$ [cf. Fig. 1(b)]. Therefore, little confining of the plasma away from the surfaces of the semiconductor walls is possible by using an axial $B$. This conclusion is also apparent because $|-\Delta E|$ never represents an appreciable percentage of $E_0$. (A much more promising method of prolonging the presence of the plasma is under investigation.[13]) The destabilizing influence of $B$ is decidedly more impressive than its stabilizing influence as evidenced by the large increments in $E$ and the steep slope $dE/dB$ which occur just beyond $B_{th}$, Fig. 1(b). These characteristics are in qualitative agreement with the nonlinear theories applicable to electron-ion plasmas.[6,7]

The present measurements of the frequency variation with $B$ confirm the early report[9] that $f$ is not a monotonic function of $B$, Fig. 3. No theory yet exists for either electron-ion or electron-hole plasmas which predicts such a property of the helical instability.

The self-$B$ produced by the helix divided by the total current, i.e., the current carried by the plasma and the initial carriers, has a maximum as a function of $B$, Fig. 4. This is qualitatively in good agreement with the electron-ion nonlinear theory.[6] No parameter, however, has been found yet which orders the data for the four samples among themselves as does the parameter pressure times radius in the electron-ion case. According to the nonlinear theory the reason for the maximum in the self-$B$ is the calculated increase in the wavelength of the helix as $B$ is raised.

The magnitude of the self-$B$ in electron-hole plasmas[1] is larger by $\sim 10^5$ than in electron-ion plasmas.[5] Related to this fact is another striking difference between the properties of the two types of plasmas. Whereas the magnitude of the paramagnetism in the supercritical region is $\sim 10$ times greater than the diamagnetism of Johnson's[5] electron-ion plasma just before $B_{th}$, the corresponding factor in the InSb plasmas[1] is $\sim 10^7$. The $10^7$ factor results from the very small diamagnetic moment of electron-hole plasmas[14] and the very large self-$B$ of the electron-hole helices.

Another way of comparing the two types of plasmas is afforded by Fig. 5. The percentage of the hysteresis fields with respect to their threshold fields range up to 55% in both the cases of the $E$ and $B$ fields. No comparable data is available yet for electron-ion plasmas but the nonlinear theory[6] suggests smaller values, $\sim 15\%$ in $E$ and $\sim 3\%$ in $B$ as maximum values. The ratio of $E_{hys}/E_{th}$ to $B_{hys}/B_{th}$, according to Fig. 5, lies between 1:1 and 2:1, whereas the typical ratio which emerges from the existing theory is $\sim 5:1$.

The occurrence of two magnetic-field thresholds as $dB/dt$ is increased, Fig. 9, suggests qualitative agreement with the theory of the helical instability in the positive column which includes the influence of time-dependent $B$. Johnson and Jerde (Fig. 4, Ref. 11) have shown that $B_{th}$ is a double-valued function of a quantity proportional to $dB/dt$. Their assumptions are so inapplicable to electron-hole plasmas, however, that comparison is not possible. It is not clear from their theory or experiments what happens if the application of a $dB/dt$ causes the plasma to pass through the unstable region of their curves, thus crossing a boundary from stable to unstable regions and then unstable to stable. The results of Fig. 12 are, to the author's knowledge, the first to probe this question in either electron-ion or electron-hole plasmas.

These results show that the instability does not cease until an appreciably smaller $B$ is reached than the $B$ which produces the onset. Certainly a $|-dB/dt|$ is not useful in stabilizing the plasma. The results of Fig. 9 suggest that $+dB/dt$ also cannot stabilize a plasma if it must traverse an unstable region to arrive at a stable one.

## V. CONCLUSION

There are several areas of qualitative agreement among the nonlinear properties of the helical instability in electron-ion and electron-hole plasmas. These include (1) a similar dependence of $E$ on $B$ throughout the range of $B$ up to several times $B_{th}$; (2) regions of a linear increase in frequency as a function of $B$; (3) turbulent behavior under highly supercritical conditions; (4) the form of the dependence of the helix self-$B$ on the applied $B$; and (5) the occurrence of two magnetic-field thresholds in a constantly increasing $dB/dt$.

Some nonlinear properties of electron-hole plasmas appear to be unique: (1) the relatively very large self-magnetic fields produced by the helical instability and (2) the nonmonotonic dependence of frequency on the applied magnetic field.

## ACKNOWLEDGMENTS

The author is grateful to Dr. James E. Drummond for many helpful discussions and suggestions. Michael F. Berg and Robert W. Boice have provided invaluable technical aid.

[13] B. Ancker-Johnson, in Proceedings of the International Conference on Physics of Semiconductors, Paris, 1964 (to be published).
[14] A. R. Moore and J. O. Kessler, Phys. Rev. 132, 1494 (1963).